Observation of Atomiclike Electronic Excitations in Pure ^{3}He and ^{4}He Clusters Studied by Fluorescence Excitation Spectroscopy

K. von Haeften,* T. Laarmann, H. Wabnitz, and T. Möller

Hamburger Synchrotronstrahlungslabor HASYLAB at Deutsches Elektronen Synchrotron DESY, Notkestrasse 85, 22603 Hamburg, Germany

(Received 25 January 2001; published 24 September 2001)

The structure of the electronically excited states of ^{3}He and ^{4}He clusters is investigated using fluorescence excitation spectroscopy. Distinct bands are observed energetically close to atomic $1s$-ns, nd, np transitions and attributed to perturbed excited He atomiclike states with different principle and orbital quantum numbers. The line shifts and widths of the bands of ^{3}He and ^{4}He clusters of the same size are different and correlate with the average particle density inside the clusters calculated using the density functional method.

DOI: 10.1103/PhysRevLett.87.153403 PACS numbers: 36.20.Kd, 71.35.–y, 73.22.–f, 78.40.Dw

Liquid ^{3}He and ^{4}He clusters are known to exhibit many fascinating properties such as superfluidity of ^{4}He clusters [1] or a strongly isotope dependent density. Because of the simple closed-shell-electronic structure of He atoms these extraordinary clusters are also interesting systems to investigate how the electronically excited states evolve from the atom to the bulk.

Unfortunately, for ^{4}He clusters and bulk liquid ^{4}He our knowledge about the excited levels and the optical properties is fairly limited. Only some experimental and theoretical studies have been performed [2–4]. In the case of ^{3}He comparable investigations do not exist. Usually, in solid or liquid systems isotopic substitution does not have much effect on the optical spectra. However, in He the situation is expected to be different. The density of liquid ^{3}He is 25% smaller than that of liquid ^{4}He and according to theoretical work [3,5] it is therefore expected that this will have a considerable effect on the optical absorption. Moreover, in the unique case of He, clusters of different size have also different average particle densities. Surface atoms of He clusters are very loosely bound and have relatively large internuclear separations compared to the bulk. Small He clusters which contain mainly surface atoms have therefore a significantly lower average density. Therefore, with control over the cluster size and the isotopic composition one has two independent parameters to explore the effect of the density on the excited levels. Our study compares the fluorescence excitation spectra of ^{3}He and ^{4}He clusters as a function of both the cluster size and the isotopic composition. Moreover, we report the first fluorescence spectra of ^{3}He and ^{4}He clusters in the visible and near infrared range (VIS/IR) which are very sensitive to features at higher energies.

Photoexcited He clusters emit an intense spectrum in the vacuum-ultraviolet (VUV) region due to transitions to the ground state. To a good approximation, the VUV fluorescence yield is proportional to the photoabsorption, because nonradiative decay to the ground state is inefficient in rare gas clusters [6]. He clusters also emit luminescence in the VIS/IR [7]. This luminescence is due to transitions between electronically excited states of He atoms and molecules formed inside He clusters after photoexcitation.

The experimental setup is described in detail elsewhere [4,6,7]. It has been modified to allow the production of ^{3}He clusters with simultaneous detection of luminescence in the VIS/IR and VUV regions. Briefly, He clusters are produced by expanding He gas at a pressure of 40 bars for ^{4}He and 7 bars for ^{3}He, respectively, through a nozzle with 5 μm diameter at temperatures between 7 and 32 K into the vacuum. For producing ^{3}He clusters the expensive gas is continuously recycled. The cluster size is determined by a comparison with results from a crossed beam scattering experiment for which similar expansion conditions have been used [8,9]. Although the production technique of ^{3}He clusters is in principle not different from ^{4}He, the size of clusters produced under similar conditions differs noticeably [9,10]. Since the ^{3}He dimer is unstable the production of *small* ^{3}He clusters ($N < 1000$) seems to be impossible by expansion from the gas phase.

One to two mm downstream from the nozzle the clusters cross the beam of monochromatized synchrotron radiation. The photon energy is varied between 20–25 eV at a resolution of 0.5 Å which corresponds to ~20 meV on average. The VUV fluorescence yield of the clusters is measured using a photomultiplier (Valvo, XP2020) covered with sodium salicylate to convert the VUV photons into the visible spectral range (sensitivity range: ~30–300 nm). In order to detect the VIS/IR luminescence a Peltier cooled photomultiplier (Hamamatsu, R943) has been installed (sensitivity range: ~300–850 nm).

The VUV luminescence yield proportional to the photoabsorption of ^{3}He and ^{4}He clusters with an average size of 10^4 atoms is displayed in Fig. 1(a). The VIS/IR-luminescence yield shown in Fig. 1(b), below, will be discussed in detail later. In the VUV fluorescence yield spectra of ^{3}He and ^{4}He clusters two prominent bands, labeled A and B, are observed. Although the shape of

 © 2001 The American Physical Society

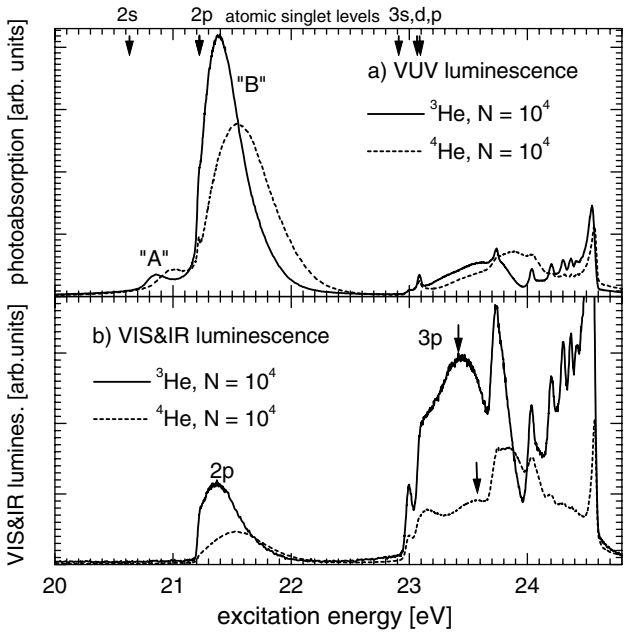

FIG. 1. Photoexcitation spectrum of ^{3}He and ^{4}He clusters showing (a) the VUV fluorescence yield (corresponding to photoabsorption) and (b) the VIS/IR yield. The nozzle temperatures were 8.8 K (^{3}He) and 14.5 K (^{4}He), respectively. The average size of both clusters is $N = 10^4$. The He atomic levels are indicated with small arrows at the top.

these bands is similar they have different peak energies and widths. For ^{3}He both the maximum energy and the widths of bands A and B are smaller than for ^{4}He clusters (see Table I). In addition, the intensity ratio between bands A and B is considerably larger for ^{4}He than for ^{3}He clusters. Bands similar to our bands A and B were observed in early studies of the VUV reflection of bulk liquid ^{4}He [2], the VUV absorption [11], and electron-energy-loss spectroscopy of ^{4}He bubbles enclosed in metal films [12–14]. The features can best be understood in the framework of perturbed atomic states. Molecular potential curves of He_2 [15] can serve as a guideline for the interpretation because the internuclear separation in liquid He clusters is rather large as a result of the low particle density. This means that all molecular transitions are blueshifted with respect to the corresponding atomic dissociation limits as the excited state potential curves are repulsive at large internuclear separation [15,16]. Moreover, transitions which are dipole forbidden for the atom become allowed in the molecule [17]. Accordingly, bands A and B are assigned to the atomic $2s^1S \leftarrow 1s^1S$ and $2p^1P \leftarrow 1s^1S$ transitions or the corresponding molecular transitions $A\ ^1\Sigma_u^+ \leftarrow X^1\Sigma_g^+$ and $D\ ^1\Sigma_u^+ \leftarrow X^1\Sigma_g^+$, respectively. The isotope dependence of the intensity ratio between bands A and B is probably due to the different internuclear separation because the density in ^{3}He clusters is lower than in ^{4}He clusters. Band A is not observed in the VIS/IR spectrum, because the $A\ ^1\Sigma_u^+$ state is the lowest lying electronically excited state and only VUV emission is possible.

TABLE I. Transition energies, energy shifts, and widths of the bands A and B of ^{3}He and ^{4}He clusters.

	Energy (eV)		Shift (eV)		Width (eV)	
Band	A ($2s$)	B ($2p$)	A	B	A	B
He_1	20.615	21.217	0	0	0	0
$^4He_{1\times10^4}$	21.02	21.55	0.385	0.333	0.380	0.580
$^3He_{1\times10^4}$	20.87	21.38	0.255	0.163	0.220	0.385

In order to investigate independently the effect of the density and the cluster size it is useful to compare the photoabsorption spectra of ^{3}He and ^{4}He clusters having the same average particle density, but a different size. To find a suitable pair of clusters, distribution functions of the density ρ along the cluster radius r (density profiles) and the Wigner-Seitz radius r_0 (the associated hard sphere radius) of ^{3}He and ^{4}He clusters have been calculated using the density functional method [18]. In the case of small clusters, for which *ab initio* Monte Carlo simulations are also available, the density profiles $\rho(r)$ obtained with density functionals have proven to be rather accurate. The method has the advantage of being easily applicable to large clusters [19,20]. The distribution function $dN(r_0)/dr$ of the Wigner-Seitz (WS) radius r_0 is connected with the density profiles via the relations $r_0 = [3/4\pi\rho(r)]^{(1/3)}$ and $dN = \rho(r)4\pi r^2 dr$. The quantity $dN(r_0)/dr$ represents the number of atoms in the cluster with a distinct (WS) radius r_0 or internuclear separation, respectively. The average WS radius r_{av} or average density, respectively, is obtained by averaging over the $dN(r_0)/dr$ distribution function. As a result it is found that a ^{4}He cluster having an almost identical arithmetic average Wigner-Seitz radius r_0 as an $N = 10\,000$ ^{3}He cluster would have a size of 300 atoms. Figure 2 shows the density profiles calculated using the density functional method and the corresponding Wigner-Seitz radii distribution functions of these particular clusters. The profiles show that the density drops smoothly towards zero at the cluster surface. Correspondingly, r_0 is distributed over a broad range, which reflects that many atoms are loosely bound and located at surface sites. The features of the $N = 10\,000$ ^{3}He and $N = 300$ ^{4}He clusters in the spectral region of the $2p^1P \leftarrow 1s^1S$ transition (band B) are shown in Fig. 3. Band B of the $N = 300$ ^{4}He clusters is strongly asymmetric and shows a sharp line at the energy of the $2p^1P$ atomic level. This line at 21.2 eV is most likely associated with atoms in the outermost surface region of the relatively small clusters. For these atoms the perturbation is too small to lead to significant broadening with respect to the limited spectral resolution. The strong asymmetry of band B of the small ^{4}He clusters is certainly due to the broader distribution of the density and the WS radius in small clusters. However, the shift from the line at 21.2 eV to the baricenter ("center of mass") is almost identical for both clusters (see Fig. 3). This indicates that the average shift is correlated with the average

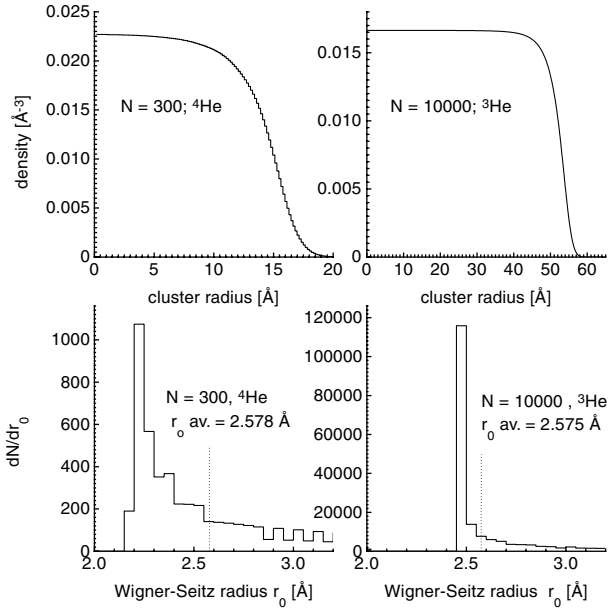

FIG. 2. Calculated density profiles and Wigner-Seitz distribution functions of ^{3}He and ^{4}He clusters having a similar *average* density, but a different size. Please, note that the WS-distribution function extends to larger values of r_0 than displayed.

Wigner-Seitz radius. We note that band *A* is barely observable for the $N = 300$ ^{4}He clusters, which is in accordance with the transition moment being lower due to the larger internuclear separation than in $N = 10\,000$ ^{4}He clusters.

Above $\geq$23 eV the differences in the excitation spectrum between the 10 000-atom-large ^{3}He and ^{4}He clusters become larger (Fig. 1). Sharp lines at the energies of the atomic n-p levels are observed. In the case of ^{3}He the lines do not appear to overlap as strongly as for ^{4}He. More important differences show up in the VIS/IR yield spectrum in Fig. 1(b). While the shape of the absorption spectrum shows only a broad feature between the energies of the atomic 3^1P (23.09 eV) and 4^1P (23.74 eV) state, the spectrum of the VIS/IR yield shows three discrete bands (Fig. 4). These bands are attributed to perturbed atomic singlet states according to the energetic position of the free atom $3s$, $3d$, and $3p$ states [21]. If our assignment is correct, it is expected that the energetic position of the $3p$ band depends on the average Wigner-Seitz radius, similar to the $2p$ features. Figure 4 shows VIS/IR excitation spectra for different cluster sizes and isotopic composition, which in turn correspond to different Wigner-Seitz radii. The $3p$ related band is indicated by an arrow. Interestingly, the position of the maximum and the shift with regard to the atomic $3p\,^1P$ level increases with the cluster size. This is in striking contrast to the findings for heavy rare gas clusters, where the transition energy decreases with cluster size [22]. Results for ^{4}He clusters which have an average WS radius larger than 2.44 Å are not shown because in this case the $3s$ and $3d$ bands become weak and the three bands merge to a single feature. The dependence of the $3p$ energy shift on the average WS radius calculated for each cluster size is illustrated in Fig. 5. The $3p$ shift is an almost monotonic function of the WS radius. The shift measured for large ^{3}He clusters matches with the extrapolated function of the ^{4}He shift which underlines

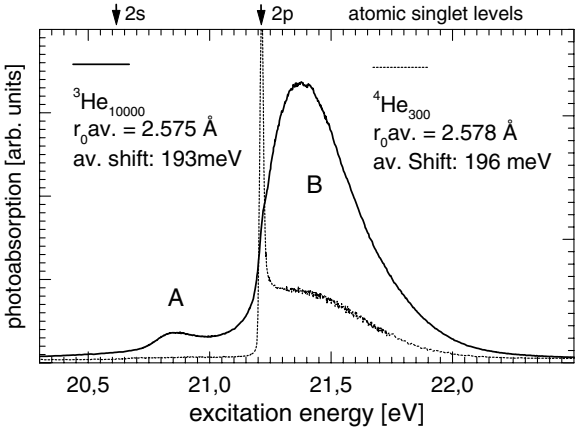

FIG. 3. Fluorescence excitation spectra in the energy range of the $2p$ excitation of ^{3}He and ^{4}He clusters with a similar average particle density. The energetic position is nearly identical for both clusters.

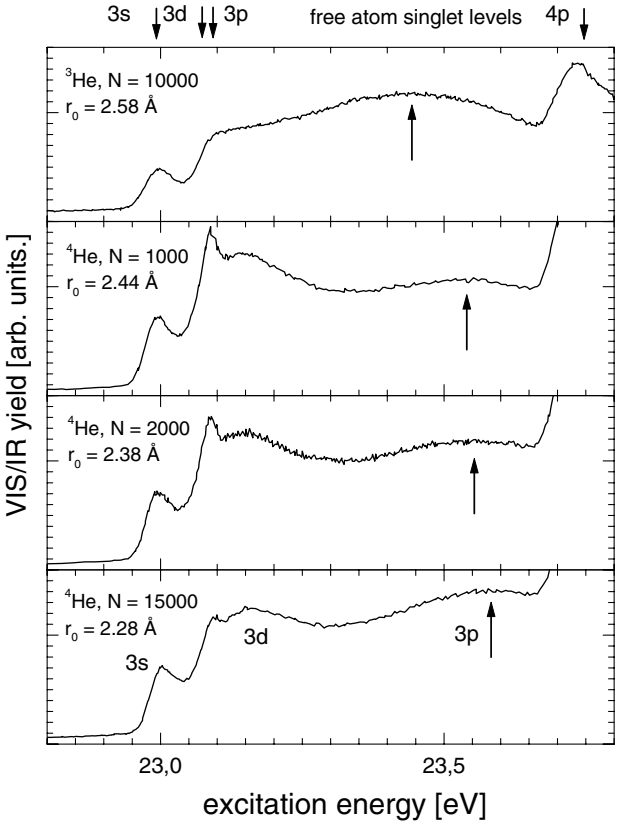

FIG. 4. VIS/IR excitation spectrum of ^{3}He and ^{4}He clusters showing the dependence of the energy of the $3p$ band (large arrow) on the cluster size and isotopic constitution connected with a different Wigner-Seitz radii r_0.

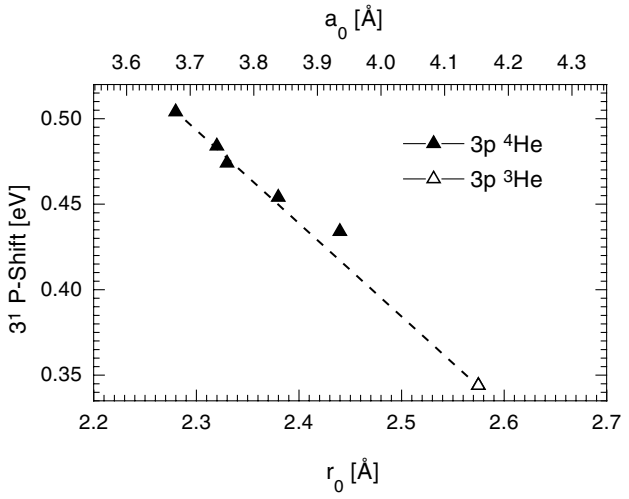

FIG. 5. Dependence of the energy of the $3p$ band shift on the average WS radius r_0 and the corresponding internuclear separation a_0, which is derived from the cluster size.

the proposed connection between the $3p$ shift and the WS radius.

Our findings for the $2p$ and $3p$ excited states suggest that the energies of the electronically excited states of He clusters depend on the density and the molecular interaction potential. This is typical of a dense gas of He atoms [16]. The energetic shift of the $3p$ state is larger than for the $2p$ state [15,16]. This is somewhat unexpected, since the repulsive part of the potential curve connected with the $2p$ state atoms is steeper than that of the $3p$ state [15]. On the other hand, a strong perturbation and a large spectral shift is reasonable taking into account that the size of the excited electron orbital is comparable to the internuclear separation in the cluster.

In conclusion we have recorded VUV fluorescence excitation spectra of ^{3}He clusters and the VIS/IR fluorescence yields of ^{3}He and ^{4}He clusters for the first time. The observed features strongly depend on the isotopic constitution. From the observation of distinct maxima in the VIS/IR excitation spectra the features could be assigned to perturbed atomiclike features with well-defined principle and orbital quantum numbers. The transition energies are blueshifted with respect to the free atom levels due to the repulsive interaction between electronically excited He atoms and ground state neighbors. In contrast to heavy rare gas clusters the shift becomes larger with increasing cluster size. The transition energies and the bandwidths indicate that the strength of perturbation is mainly controlled by the particle density. A correlation of the $2p$ and the $3p$ energy shift with the average particle density is observed.

We are grateful to Manuel Barranco, Universitat de Barcelona, Franco Dalfovo, Universitá Cattolica di Brescia, and Jan Harms, Max-Planck-Institute for Strömungsforschung for many fruitful discussions, calculating density profiles, and the communication of unpublished material. Financial support from the DFG under Grants No. Mo 719/1-2 and No. Mo 719/1-3 is kindly acknowledged.

*Present address: Lehrstuhl für Physikalische Chemie II, Ruhr-Universität Bochum, 44780 Bochum, Germany.
Email address: klaus.von.haeften@ruhr-uni-bochum.de

[1] S. Grebenev, J. P. Toennies, and A. F. Vilesov, Science **279**, 2083 (1998).
[2] C. M. Surko, G. J. Dick, F. Reif, and W. C. Walker, Phys. Rev. Lett. **23**, 842 (1969).
[3] A. A. Lucas, J. P. Vigneron, S. E. Donnelly, and J. C. Rife, Phys. Rev. B **28**, 2485 (1983).
[4] M. Joppien, R. Karnbach, and T. Möller, Phys. Rev. Lett. **71**, 2654 (1993).
[5] Peter Taylor, Chem. Phys. Lett. **121**, 3 (1985); **121**, 205 (1985).
[6] Roland Karnbach, Malte Joppien, Jörn Stapelfeldt, Jens Wörmer, and Thomas Möller, Rev. Sci. Instrum. **64**, 2838 (1993).
[7] K. von Haeften, A. R. B. de Castro, M. Joppien, L. Moussavizadeh, R. von Pietrowski, and T. Möller, Phys. Rev. Lett. **78**, 4371 (1997).
[8] J. Harms, J. P. Toennies, and F. Dalfovo, Phys. Rev. B **58**, 3341 (1998).
[9] J. Harms (private communication).
[10] Jan Harms, Matthias Hartmann, Boris Sartakov, J. Peter Toennies, and Andrej F. Vilesov, J. Chem. Phys. **110**, 5124 (1999).
[11] S. E. Donnelly, J. C. Rife, J. M. Gilles, and A. A. Lucas, J. Nucl. Mater. **93/94**, 767 (1980).
[12] J. C. Rife, S. E. Donnelly, A. A. Lucas, J. M. Gilles, and J. J. Ritsko, Phys. Rev. Lett. **46**, 1220 (1980).
[13] S. E. Donnelly, J. C. Rife, J. M. Gilles, and A. A. Lucas, IEEE Trans. Nucl. Sci. **28**, 1820 (1981).
[14] W. Jäger, R. Manzke, H. Trinkaus, G. Crecelius, R. Zeller, J. Fink, and H. L. Bay, J. Nucl. Mater. **111/112**, 674 (1982).
[15] S. L. Guberman and W. A. Goddard, Phys. Rev. A **12**, 1203 (1975).
[16] V. Guzielski, M. C. Castex, J. Wörmer, and T. Möller, Chem. Phys. Lett. **179**, 243 (1991).
[17] Y. Tanaka and K. Yoshino, J. Chem. Phys. **50**, 3098 (1969).
[18] Jan Harms, J. Peter Toennies, M. Barranco, and Marti Pi, Phys. Rev. B **63**, 184513 (2001).
[19] J. Dupont-Roc, M. Himbert, N. Pavloff, and J. Treiner, J. Low Temp. Phys. **81**, 31 (1990); F. Dalfovo, A. Lastri, L. Pricaupenko, S. Stringari, and J. Treiner, Phys. Rev. B **52**, 1193 (1995).
[20] F. Dalfovo, Z. Phys. D **29**, 61 (1994).
[21] William C. Martin, J. Res. Natl. Bur. Stand. Sect. A **64**, 19 (1960).
[22] J. Wörmer, R. Karnbach, M. Joppien, and T. Möller, J. Chem. Phys. **104**, 8269 (1996).